Deducing ink thickness variations by a spectral prediction model

R. D. Hersch, M. Brichon, T. Bugnon, P. Amrhyn, F. Crété,
Ecole Polytechnique Fédérale de Lausanne (EPFL), Switzerland

S. Mourad, Eidgenössische Materialprüfungs- und Forschungsanstalt (EMPA), St-Gallen, Switzerland

H. Janser, Y. Jiang, M. Riepenhoff, Maschinenfabrik, Bern, Switzerland

ABSTRACT

Most existing techniques for regulating the ink flow in offset presses rely on density measurements carried out on specially printed patches. In the present contribution, we develop a methodology to deduce ink thickness variations from spectral measurements of multi-chromatic halftone patches located within the printed page. For this purpose, we extend the Clapper-Yule spectral reflectance prediction model by expressing the transmittance of the colorants composed of superposed inks as a function of the ink transmittances and of fitted ink layer thicknesses. We associate to each ink an ink thickness variation factor. At print time, this ink thickness variation factor can be fitted in order to minimize a difference metric between predicted reflection spectrum and measured reflection spectrum. The ink thickness variations deduced from multi-chromatic halftones allow to clearly distinguish between normal ink volume, reduced ink volume or increased ink volume. This information can then be used for performing control operations on the printing press.

Keywords: Color printing, color halftone, spectral reflection prediction model, dot gain, ink spreading, ink flow, ink thickness, ink density, ink flow control

1. Introduction

In order to achieve accurate color reproduction, today's printers and presses often require manual intervention. They generally do not provide automatic means for continuously adapting themselves to variations in operating conditions, such as printing speed, temperature or humidity. Specially laid out solid and halftone patches are printed, their densities are measured and are used for the manual or semi-automatic control of press actuation parameters such as ink feed [Brunner 1989].

Models for predicting the reflectance of printed halftone patches, or inversely, for deducing the surface coverages from halftone patch reflection spectra exist [Iino and Berns 1998], [Balasubramanian 1999], [Rogers 2000], [Hersch et al. 2005], [Bugnon et al. 2007], but have not been used for regulating output parameters of printers such as ink flow. The present contribution aims at proposing a spectral prediction model enhanced to predict ink thickness variations from halftone prints. Previous research aimed at adjusting the model predicting the reflection spectra of halftone patches when replacing one substrate by another substrate [Shaw et al. 2005]. For this purpose, comparisons are carried out between methods relying on Beer's law, the Kubelka-Munk theory, the Yule-Nielsen modified Spectral Neugebauer model [Yule and Nielsen 1951, Viggiano 1990] and on a regression based on principal component decomposition.

The thickness variation enhanced spectral prediction model we propose relies on the Clapper-Yule model [Clapper and Yule 1953]. In contrast to the Yule-Nielsen modified Neugebauer model, the Clapper-Yule spectral prediction model incorporates explicitly the transmittance of the inks. In order to provide accurate predictions, the Clapper-Yule model has been enhanced to account for ink spreading according to the different ink halftone superposition conditions [Hersch, et al., 2005].

We introduce ink thicknesses by expressing the transmittance of the colorants (ink colors and overprint colors,

also known as Neugebauer primaries) as a function of the respective thicknesses of their corresponding ink layers. This enables transforming the Clapper-Yule spectral prediction model into a thickness enhanced spectral prediction model incorporating as parameters the initial thicknesses of the inks. By incorporating a multiplicative factor for each of the ink thicknesses, we obtain for each ink a factor expressing its thickness variation, i.e. its thickness increase or decrease. Ink thickness variation factors are obtained by minimizing a difference metric between predicted reflection spectrum and measured reflection spectrum.

It is well known that dark color tones, dark gray or black can be generated either by superposing similar amounts of cyan, magenta, yellow or by printing a certain amount of pure black ink. Accordingly, a darker halftone may be created by similar thickness increases of the cyan, magenta and yellow inks or by a thickness increase of the black ink. The issue is resolved by considering reflection spectra comprising both the visible wavelength range, i.e. from 380nm to 730nm, and the near infra-red wavelength range, i.e. from 730nm to 850nm [Wang & Nemeth 1995, Bugnon & Hersch 2007]. In the near-infrared wavelength range, for the considered inks, the cyan, magenta and yellow colorants do not absorb light. Only the pigmented black ink absorbs light. An ink thickness variation model with a wavelength range from 380 nm to 850 nm, i.e. comprising the visible and near-infrared wavelength ranges, enables computing unambiguously thickness variations for the cyan, magenta, yellow and black inks.

The developed ink thickness variation prediction model has been verified on 1529 different test patches printed by a WIFAG web offset press on uncoated newsprint paper. Both the reference sheet and the test sheets comprise 48 calibration patches and 1529 test patches. The test sheets are printed with many variations of ink thicknesses, either of a single ink, or independent thickness variations of 2, 3 or 4 inks. The reflectance spectrum of each of the test patches is measured and corresponding ink thickness variations are fitted by minimizing a metric expressing the difference between the predicted reflection spectrum and the measured reflection spectrum. The deduced thickness variations allow to establish the mean ink thickness variation of a given test print as well as its standard deviation. It is possible to feed the mean ink thickness variation factors back into the spectral prediction model and measure its prediction accuracy. This gives a quality assessment of the deduced thickness variation factors.

The spectral measurements are carried out with a Datacolor MF45 NIR spectrophotometer having a $45^o/0^o$ geometry, i.e. a D65 light source illuminating the printed sample at an angle of 45^o and a sensor capturing the reflected spectrum at 0^o (normal to the printed sample). The acquired reflection spectra range from 380nm to 1100nm. Only the range 380nm to 850nm is used in the present experiments.

In Section 2, we introduce the classical Clapper-Yule spectral prediction model and in Section 3 the ink spreading enhancement accounting for ink spreading in all superposition conditions. In Section 4, we introduce the ink thickness equations and in Section 5 the ink thickness variation factors, which are inserted into the Clapper-Yule model. In Section 6, we describe the calibration of the system. In Section 7, we describe the experiments and show the results. In Section 8, we draw the conclusions.

2. The Clapper-Yule based spectral prediction model

Among the classical color prediction models [Wyble and Berns 2000], only the Clapper-Yule model [Clapper and Yule 1953] supports halftones and accounts for the multiple internal reflections occurring at the interface between the print and the air.

For introducing the Clapper-Yule model, we consider a single halftone ink layer with a fractional surface coverage a printed on a coated paper substrate (Fig. 1). Incident light has the probability a of reaching the paper substrate by passing through ink of transmittance $t(\lambda)$ and a probability $(1-a)$ of reaching the substrate without traversing the ink layer. Since r_s is the specular reflection at the air-paper interface, only portion $(1-r_s)$ actually enters the coated paper. The light reaching the paper substrate is attenuated by a factor $(1-r_s)$ $(1-a+at)$, with $(1-a+at)$ representing the attenuation of light by passing once through the halftone ink layer. Light is then laterally scattered and diffusely reflected by the paper substrate according to the paper substrate reflectance $r_g(\lambda)$. Traveling upwards, it traverses the print with a portion a traversing the ink and a portion $(1-a)$ traversing an area free of ink. It is reflected at the print-air interface according to a reflection factor r_i, representing the Fresnel reflectivity integrated over all incident angles. The non-reflected part $(1-r_i)$ of the light exits. At the first exit, the spectral attenuation of the incident light is therefore $(1-r_s)\ r_g(1-r_i)\ (1-a+at)^2$.

The part reflected at the coated paper-air interface travels downward, is diffusely reflected by the paper and travels upwards again. At the second exit, the spectral attenuation is $(1-r_s)\, r_g(1-r_i)\, (1-a+at)^2\, r_i\, r_g\, (1-a+at^2)$.

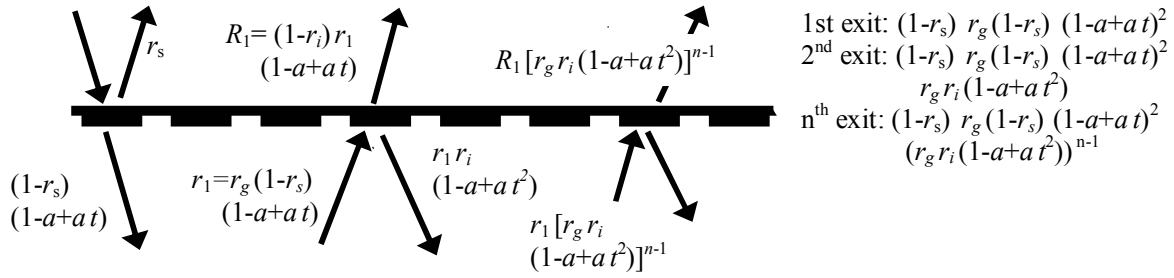

Figure 1. Attenuation of light by multiple reflections on a halftone printed patch

With K giving the fraction of specular reflected light reaching the photospectrometer, and by considering the light emerging after 0, 1, 2,..., n-1 internal reflections (Fig. 1), we obtain the reflection spectrum

$$R(\lambda) = K \cdot r_s + (1-r_s) \cdot r_g (1-r_i) \cdot (1-a+a \cdot t)^2 \cdot (1 + r_i \cdot r_g (1-a+a \cdot t^2) + (r_i \cdot r_g (1-a+a \cdot t^2))^2 + \ldots + (r_i \cdot r_g (1-a+a \cdot t^2))^{n-1}) \quad (1)$$

For an infinite number of emergences, Eq. (1) yields a geometric series. We obtain the well-known Clapper-Yule expression

$$R(\lambda) = K \cdot r_s + \frac{(1-r_s) \cdot r_g \cdot (1-r_i) \cdot (1-a+a \cdot t)^2}{1 - r_g \cdot r_i \cdot (1-a+a \cdot t^2)} \quad (2)$$

The light components that have been summed up in Eqs. (1) and (2) are fractions of the incident irradiance. Therefore, Eq. (5) expresses a reflectance, i.e. the ratio between exiting irradiance and incident irradiance. Ideally, incident and exiting irradiances should be measured with a spectrophotometer having an integrated sphere geometry. However, the exact expression for the spectral reflectance factor predicted according to a $45^o/0^o$ measuring geometry [Hersch et al, 2005] is numerically very similar to expression (2). One may therefore, in the context of color reproduction, carry out all measurements with a photospectrometer having a $45^o/0^o$ geometry, i.e. an instrument where light illuminates the printed sample at an orientation of 45 degrees and where reflected light (radiance) is captured at an orientation normal to the sample. For such a geometry, no specular reflection component is captured by the photospectrometer, i.e. K=0.

In the case of paper printed with 3 independently laid out ink halftone layers such as cyan, magenta and yellow of respective surface coverage c, m and y, the surface coverages a_j of the resulting 8 basic colorants, i.e. white (a_w) , cyan (a_c), magenta (a_m), yellow (a_y), red (a_r), green (a_g), blue (a_b) and black (a_k) are obtained according to the Demichel equations [Demichel 1924]:

$$\begin{aligned} &a_c = c \cdot (1-m) \cdot (1-y); \quad a_m = (1-c) \cdot m \cdot (1-y); \quad a_y = (1-c) \cdot (1-m) \cdot y \\ &a_r = (1-c) \cdot m \cdot y; \quad a_g = c \cdot (1-m) \cdot y; \quad a_b = c \cdot m \cdot (1-y); \\ &a_k = c \cdot m \cdot y; \quad a_w = (1-c) \cdot (1-m) \cdot (1-y) \end{aligned} \quad (3)$$

The Demichel equations can be extended to 4 or more inks [Hersch et. al. 2005].

By inserting the surface coverages of colorants a_j and their transmittances t_j in equation (2), we obtain for the predicted reflectance of a color patch printed with combinations of cyan, magenta and yellow inks

$$R(\lambda) = K \cdot r_s + \frac{(1-r_s)\cdot r_g \cdot (1-r_i)\cdot \left(\sum_{j=1}^{8} a_j \cdot t_j\right)^2}{1-r_g \cdot r_i \cdot \sum_{j=1}^{8} a_j \cdot t_j^2} \tag{4}$$

Both the specular reflection r_s and the internal reflection r_i at the paper-air interface depend on the refraction indices of the air (n_0=1) and of the print (n_1=1.53), independently of whether the considered surface is white or printed (the ink is located within the coated paper surface). According to the Fresnel equations [Hecht 1974], for collimated light at an incident angle of 45°, the specular reflection factor is r_s=0.054. With light diffusely reflected by the paper (Lambert radiator), by summing up the contributions at all incident angles [Hebert and Hersch 2004], we obtain the internal reflection factor r_i. For coated paper, r_i=0.614. Values of r_i for different indices of refraction are tabulated by Judd [1942] and by Emmel [2003].

To put the model into practice, we deduce from Eq. (2) the intrinsic reflectance spectrum r_g of a blank paper by setting the ink coverage a=0, and by measuring R_w , the blank paper reflectance.

$$r_g = \frac{R_w - K \cdot r_s}{1+(1-K)\cdot r_i \cdot r_s + r_i \cdot R_w - r_s - r_i} \tag{5}$$

We then extract the transmittance of the colorants, i.e. the individual solid inks and solid ink superpositions t_w, t_c, t_m, t_y, t_r, t_g, t_b, t_k by inserting in Eq. (2) as $R(\lambda)$ the corresponding measured solid (100%) colorant reflectance R_i and by setting the ink coverage a=1.

$$t_i = \sqrt{\frac{R_i - K \cdot r_s}{r_g \cdot r_i \cdot (R_i - K \cdot r_s) + r_g \cdot (1-r_i)\cdot (1-r_s)}} \tag{6}$$

When deriving the Clapper-Yule model, we assumed that the probability to exit from an ink dot is proportional to the ink dot surface coverage, independently if the incident light crosses the print surface through an ink dot or through a white space. This is correct when lateral propagation of light is important in respect to the screen element period. Experiments showed that the Clapper-Yule model makes accurate spectral predictions at screen frequencies equal or larger than 150 lines per inch (coated paper, offset). For newsprint paper, it makes accurate predictions at screen frequencies starting from 100 lines per inch. At lower screen frequencies, it is necessary to extend the original Clapper-Yule model. A simple recently proposed extension, consists in having a weighted mean between the original Clapper-Yule model and a Saunderson corrected Neugebauer model [Saunderson 1942], i.e. a Neugebauer model [Neugebauer 1937], where internal reflections between the paper bulk and the print-air interface are accounted for [Hersch and et al, 2005].

$$R(\lambda) = K \cdot r_s + (1-r_s)\cdot r_g \cdot (1-r_i)\cdot \left[b \cdot \left[\sum_{j=1}^{8} \frac{a_j \cdot t_j^2}{1-r_i \cdot r_g \cdot t_j^2} \right] + (1-b) \cdot \frac{\left(\sum_{j=1}^{8} a_j \cdot t_j\right)^2}{1-r_g \cdot r_i \cdot \sum_{j=1}^{8} a_j \cdot t_j^2} \right] \tag{7}$$

The part weighted by (1–b) is the Clapper-Yule component and the part weighted by b is the Saunderson corrected Neugebauer component.

3. The ink spreading equations

Equations (4), respectively (7) provide a full spectral prediction mo

del if the effective colorant surface coverages are known. In the general case however, the nominal ink surface coverages (also called "digital counts") are given, from which, according to the Demichel equations (3), only the nominal colorant surface coverages can be deduced. Due to ink spreading (mechanical dot gain), effective surface coverages (u_{eff}) are generally larger than the nominal surface coverages (u_{nom}). The effective surface coverage of a halftone dot depends on whether it is printed on paper, in superposition with another ink or in superposition with two inks. It is therefore necessary to establish the tone reproduction curves, i.e. the functions mapping nominal surface coverages to effective surface coverages for each halftone ink in each superposition condition.

In the case of 3 inks, we have 12 superposition conditions: each ink halftone alone on paper (one per ink–>3), each ink halftone on top of another solid ink (two per ink halftone –> 6) and each ink halftone on top of two solid inks (one per ink halftone –>3). We would like to establish in each superposition condition the function mapping nominal to effective surface coverages. At no surface coverage (0%) and at full surface coverage (solid 100%), nominal and effective surface coverages are identical. We select patches printed at specific nominal surface coverages (e.g. 25%, 50%, 75%) and fit the corresponding effective surface coverages by minimizing a difference metric (e.g. the sum of square differences) between measured and predicted reflection spectra. By interpolating between the points (u_{nom},u_{eff}) (e.g linear interpolation), one obtains in each superposition condition s a function $f_s(u_{nom})$ mapping nominal to effective surface coverages. Figure 2 shows the corresponding dot gain curves, i.e. the effective surface coverage minus the nominal surface coverage, as a function of the nominal surface coverage, for the cyan, magenta and yellow inks, in each superposition condition.

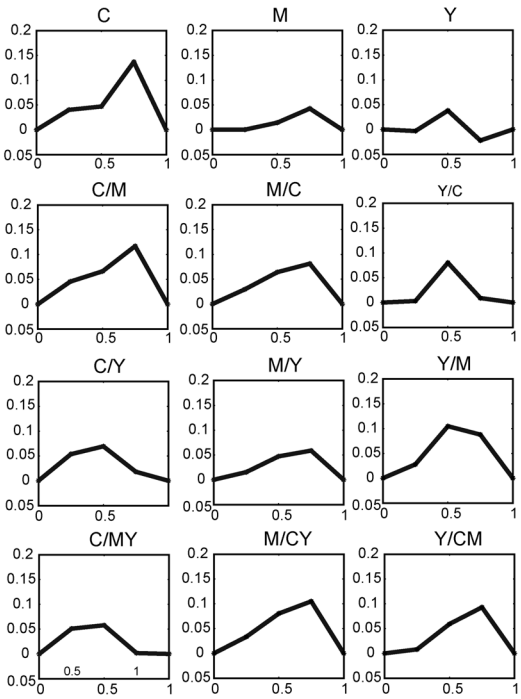

Figure 2. Dot gain curves, representing effective minus nominal surface coverages, with effective surface coverages fitted on patches printed at 25%, 50% and 75% nominal surface coverages, for a web offset print on newsprint paper, at a screen frequency of 100 lpi.

For the three inks i_c, i_m and i_y, the superposition conditions s are cyan alone (c), cyan superposed with magenta (c/m), cyan superposed with yellow (c/y), cyan superposed with magenta and yellow (c/my); magenta alone (m), magenta superposed with cyan (m/c), magenta superposed with yellow (m/y), magenta superposed with

cyan and yellow (*m/cy*), yellow alone (*y*), yellow superposed with cyan (*y/c*), yellow superposed with magenta (*y/m*) and yellow superposed with cyan and magenta (*y/cm*).

In order to obtain the effective surface coverages *c*', *m*' and *y*' of a color halftone patch, it is necessary, for each ink i_u, to weight the contributions of the corresponding mapping functions f_u, $f_{u/v}$, $f_{u/w}$, and $f_{u/vw}$ according to the surface coverages of the corresponding colorants. For the considered system of inks i_c, i_m and i_y with nominal coverages *c*, *y* and *m* and effective coverages *c*', *m*' and *y*', assuming that inks are printed independently of each other, by computing the relative weight, i.e. the relative surface of each underlying colorant, we obtain the system of equations (8). In analogy with Demichel's equations (3), the proportion (relative effective surface) of a halftone patch printed with ink *cyan* of coverage *c* on paper white is (1- *m*') (1- *y*'). The proportion of the same patch printed on top of solid ink *magenta* is *m*' (1-*y*'), the proportion of the same patch printed on top of solid ink *yellow* is (1-*m*') *y*' and the proportion of the same patch printed on top of solid inks *magenta* and *yellow* is *m*' *y*'. We obtain the following system of equations:

$$
\begin{aligned}
c' &= f_c(c)\,(1-m')\,(1-y') + f_{c/m}(c)\,m'\,(1-y') + f_{c/y}(c)(1-m')\,y' + f_{c/my}(c)\,m'\,y' \\
m' &= f_m(m)\,(1-c')\,(1-y') + f_{m/c}(m)\,c'\,(1-y') + f_{m/y}(m)(1-c')\,y' + f_{m/cy}(m)\,c'\,y' \\
y' &= f_y(y)\,(1-c')\,(1-m') + f_{y/c}(y)\,c'\,(1-m') + f_{y/m}(y)(1-c')\,m' + f_{y/cm}(y)\,c'\,m'
\end{aligned}
\qquad (8)
$$

This system of equations can be solved iteratively: one starts by setting initial values of *c*', *m*' and *y*' equal to the respective nominal coverages *c*, *m* and *y*. After one iteration, one obtains new values for *c*', *m*' and *y*'. These new values are used for the next iteration. After a few iterations, typically 4 to 5 iterations, the system stabilizes and the obtained coverages *c*', *m*' and *y*' are the effective coverages. The system of equations (8) allows us therefore to compute the effective ink dot surface coverages resulting from the combination of elementary ink surface coverages present in different superposition conditions. The effective colorant coverages a_c', a_m', a_y', a_r', a_g', a_b' a_k', a_w' are obtained from the effective dot surface coverages *c*', *m*' and *y*' of the inks according to the Demichel equations (Eq. 3)**.** The complete model comprising ink spreading in all superposition conditions for the cyan, magenta and yellow inks is illustrated in Figure 3. The model can be extended to the 4 cyan, magenta, yellow and black inks in a straightforward manner.

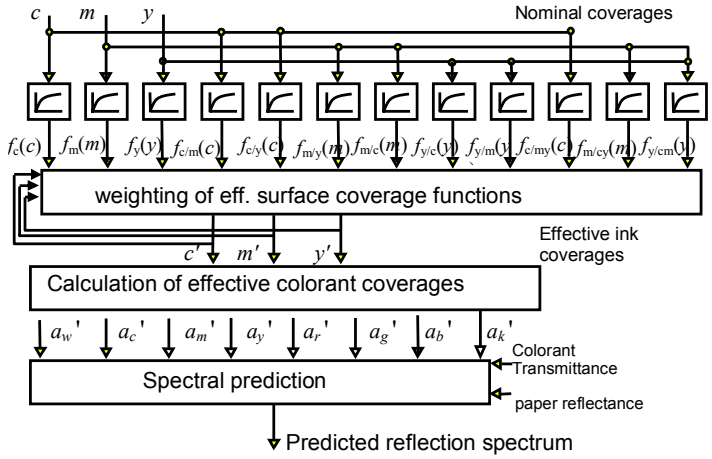

Figure 3. Spectral prediction model with ink spreading in all superposition conditions

The use of the ink spreading model together with the spectral prediction model is necessary in order to achieve a high prediction accuracy. Table 1 shows the prediction accuracies for 317 cyan, magenta and yellow halftone patches (*cmy*) and for 1529 cyan, magenta, yellow and black patches (*cmyk*), with and without the full ink spreading model. Prediction accuracies are expressed as ΔE_{94} color differences between predicted color and measured color, calculated from the corresponding reflection spectra. The reference accuracy is based on a single ink dot gain optimization model [Balasubramanian 1999], noted "single ink dot gain".

Table 1. Prediction accuracy improvement due to the ink spreading model, tested on a typical print (Table 4, print C+) with 317 cyan, magenta and yellow halftone patches (*cmy*) and 1529 cyan, magenta, yellow and black patches (*cmyk*).

Offset 100 lpi, web offset on newsprint paper	Mean ΔE_{94}		Max ΔE_{94}		% of patches with ΔE_{94} >3	
	cmy	*cmyk*	*cmy*	*cmyk*	*cmy*	*cmyk*
Single ink dot gain	1.71	2.00	4.20	6.05	7.5%	14%
Full ink spreading	1.24	1.30	3.31	5.56	1.5%	2%

Since ink thickness variations are obtained by a fitting process, it is important that all other elements of the spectral prediction model enable the model to provide accurate spectral predictions. When this is not the case, as for example in the case of a single ink dot gain, the deduced ink thickness variations represent "artefacts" that improve the prediction accuracy, i.e. the increased or decreased ink thicknesses compensate for the prediction inaccuracies of the spectral prediction model.

4. Expressing colorant transmittances by ink transmittances and ink thicknesses

Our aim is to deduce ink thickness variations. According to Beer's law, for non-scattering inks, when increasing the thickness of an ink of transmittance $t(\lambda)$ by a factor d, one obtains a transmittance $t(\lambda)^d$. Let us first express the transmittance of the composed colorants, i.e. the colorants formed by superpositions of one or more inks as a function of the transmittances of their contributing inks. Then, we may deduce ink thickness variations by introducing for each ink a scalar multiplicative factor in the exponent of its corresponding ink transmittance. This scalar multiplicative factor, called ink thickness variation, is then fitted by minimizing a difference metric between the reflection spectrum predicted according to the ink thickness extended spectral model and the measured reflection spectrum of a patch incorporating the corresponding ink halftones.

Let us establish the equations allowing us to calculate the initial thicknesses of the inks, for all the colorants. For colorants formed by a single ink, the initial thicknesses are one, since their transmittance have directly been deduced from the spectral prediction model according to formula (6). The transmittance of a colorant *AB* formed by two inks *A* and *B* is equal to the multiplication of their thickness adapted respective transmittances. The same applies for 3 or more inks.

$$t_{AB} = t_A^{d_{Ab}} \cdot t_B^{d_{aB}} \; ; \qquad t_{ABC} = t_A^{d_{Abc}} \cdot t_B^{d_{aBc}} \cdot t_C^{d_{abC}} \tag{9}$$

Exponent d_{Ab}, respectively d_{aB} express the thicknesses of ink *A* in the superposition of inks *A* and *B* and of ink *B* in the superposition of inks *A* and *B*, respectively. An analog notation is used for three and more inks.

For the colorants formed by cyan, magenta and yellow inks, the transmittances of the colorants as a function of the transmittances and of the initial thicknesses of their constituting inks are

$$\begin{aligned} &t_C = t_C^{d_C} \quad ; \quad t_M = t_M^{d_M} \quad ; \quad t_Y = t_Y^{d_Y} \\ &t_{CM} = t_C^{d_{Cm}} \cdot t_M^{d_{cM}} \\ &t_{CY} = t_C^{d_{Cy}} \cdot t_Y^{d_{cY}} \\ &t_{MY} = t_M^{d_{My}} \cdot t_Y^{d_{mY}} \\ &t_{CMY} = t_C^{d_{Cmy}} \cdot t_M^{d_{cMy}} \cdot t_Y^{d_{cmY}} \end{aligned} \tag{10}$$

Note that initial thicknesses d_C, d_M, d_Y are 1 if the patches from which the thicknesses is deduced are the same as the ones from which the transmittances of the inks are deduced. The scalar initial thicknesses $d_C, d_M, d_Y, d_{Cm}, d_{cM}, d_{Cy}, d_{cY}, d_{My}, d_{mY}, d_{Cmy}, d_{cMy}, d_{cmY}$ are deduced by minimizing a difference metric between the predicted and measured reflection spectra (for example, by using Matlab's *fmincon* constrained optimization function).

The respective relative thicknesses of the inks for the different colorants formed by cyan, magenta and yellow inks are shown in Table 2. These relative thicknesses are deduced from reflectance spectra of solid colorant patches printed by a WIFAG web offset press at 100 lpi on uncoated newsprint paper. The considered visible wavelength range is 380-730 nm. Very similar thicknesses are obtained by considering an extended wavelength range from 380 to 850nm.

Table 2. Respective relative ink thicknesses of the cyan, magenta and yellow ink, for the blue (cyan+magenta), green (cyan+yellow), red (magenta+yellow) and chromatic black (cyan+magenta+yellow) colorants (reference print K+, Table 4). Inks are printed in the order cyan, magenta and yellow.

cyan	**mag**	**yel**	**red**		**green**		**blue**		**black**		
d_c	d_m	d_y	d_{My}	d_{mY}	d_{Cy}	d_{cY}	d_{Cm}	d_{cM}	d_{Cmy}	d_{cMy}	d_{cmY}
1	1	1	1 .127	0.509	1.148	0.782	0.976	0.801	1.122	0.679	0.537

Table 2 shows that, in the majority of cases, the superposition of two or more inks tends to reduce the ink thicknesses. This may be due to several reasons. In real web offset prints, the inks are not really superposed, but, since they are printed wet on wet, they tend to penetrate each other. The offset process itself also does not deposit a constant amount of ink: only a portion of the ink deposited on the blanket is transferred onto paper, and that portion varies if the paper is blank or already printed with another ink. This phenomenon is called the trapping effect [Kipphan 2001, pp. 224-225].

In colorants incorporating the yellow ink, the first ink tends to be thicker and the yellow ink to be relatively thin. A more detailed analysis of the superposition spectra shows that the yellow ink is less transparent and scatters part of the light upwards towards the air. Since there is less absorption by the yellow ink, the "equivalent thickness" of the yellow ink is reduced. Why the other ink becomes thicker may be due to the mottling effect, where the inks have the tendency to form spatially distinct clusters. However, this topic deserves further research.

Table A in the Appendix shows the respective ink thicknesses for colorants incorporating the black ink. In order to distinguish between chromatic black (superposition of cyan, magenta and yellow) and pure black, we fit the ink thicknesses by considering reflection spectra ranging between 380nm and 850nm (visible + near infrared wavelength range, where only the pure black ink absorbs light).

Let us verify that the thickness enhanced spectral prediction model also works with colorant transmittances expressed according to Equations (10). Table 3 shows the prediction accuracies both for the initial spectral prediction model and for the thickness enhanced spectral prediction models. Both models rely on the Clapper-Yule model, extended by accounting for ink spreading in all superposition conditions (Section 3).

The predictions relying on the ink thickness enhanced spectral prediction model are slightly less accurate. Instead of having independent, separately measured colorant transmittances, i.e. for 3 inks a total of 8 colorant transmittances and for 4 inks a total of 16 colorant transmittances, we only have the initial transmittances of the inks, i.e. 3 or 4 ink transmittances, and the fitted scalar thickness values, i.e. 12 initial thickness values for 3 inks and 32 values for 4 inks (12 values for inks *cmy* and 20 values for ink *k* superposed with inks *cmy*, Table A in Appendix).

Table 3. Prediction accuracy for a typical print (Table 4, print C+), with (a) the original colorant transmittances deduced from reflectance measurements of printed colorants and (b) with the colorant transmittances expressed as a function of the ink transmittances and of fitted ink layer thicknesses, tested on 317 cyan, magenta and yellow halftone patches (*cmy*) and on 1529 cyan, magenta, yellow and black patches (*cmyk*).

Offset 100 lpi, web offset on newsprint paper	Mean ΔE_{94}		Max ΔE_{94}		% of patches with ΔE_{94} >3	
	cmy	*cmyk*	*cmy*	*cmyk*	*cmy*	*cmyk*
(a) Spectral prediction model with "measured" colorant transmittances	1.24	1.30	3.31	5.55	1.5%	2.0%
(b) Ink thickness enhanced spectral prediction model	1.31	1.63	4.28	8.96	4.4%	9.2%

5. Deducing ink thickness variations

Ink volume variations generally occur due to a drift in the operation of the printer. Increasing or decreasing the ink flow modifies both the thickness of the ink and the surface coverage of the ink halftone. In the present contribution, we deduce variations of the amount of ink by assuming that the surface coverage of the ink halftone does not change and that only the ink thickness varies. We make the simplifying assumption that the ink volume is equal to the surface coverage multiplied by the ink thickness. We keep the surface coverages constant and deduce the ink thickness variations by minimizing a difference metric between predicted reflection spectra and measured reflection spectra. These ink thickness variations correspond to variations of the ink volumes.

In order to obtain the ink thickness variations from measured reflection spectra of a halftone, we extend formula (10) by associating to each ink thickness d_i a multiplicative ink thickness variation factor v_i. We assume that when there is a variation in the amount of an ink deposited on the print, the variation is proportionally the same for all colorants incorporating that ink. In the case of cyan, magenta and yellow inks, we obtain the following expressions for the colorant transmittances

$$
\begin{aligned}
t_C &= t_C^{d_C \cdot v_C} \\
t_M &= t_M^{d_M \cdot v_M} \\
t_Y &= t_Y^{d_Y \cdot v_Y} \\
t_{CM} &= t_C^{d_{Cm} \cdot v_C} \cdot t_M^{d_{cM} \cdot v_M} \\
t_{CY} &= t_C^{d_{Cy} \cdot v_C} \cdot t_Y^{d_{cY} \cdot v_Y} \\
t_{MY} &= t_M^{d_{My} \cdot v_M} \cdot t_Y^{d_{mY} \cdot v_Y} \\
t_{CMY} &= t_C^{d_{Cmy} \cdot v_C} \cdot t_M^{d_{cMy} \cdot v_M} \cdot t_Y^{d_{cmY} \cdot v_Y}
\end{aligned}
\qquad (11)
$$

The colorant transmittances described in Eqs. (11) are plugged as the transmittances t_j into the Clapper-Yule expression (4) or, at low screen frequency, into the extended expression (7). Corresponding effective colorant surface coverages a_j are deduced from the known nominal ink surface coverages according to expressions (8) and (3). We now have the thickness variation extended Clapper-Yule model predicting the reflection spectrum of a halftone patch from nominal surface coverages, incorporating, in the case of the three cyan, magenta and yellow inks, the corresponding ink thickness variation factors v_C , v_M , v_Y . By minimizing a difference metric between predicted and measured reflection spectra, one obtains optimal values of the thickness variation factors v_C , v_M , v_Y . In a similar manner, the whole framework can be extended to 4 inks (thickness variation

coefficients v_C , v_M , v_Y, , v_K) by considering reflection spectra both in the visible and in the near infrared wavelength range.

6. Calibration of the thickness variation enhanced spectral prediction model

Let us briefly review the steps necessary for the calibration of the thickness variation enhanced spectral prediction model. Firstly, the internal reflection of r_g of paper and the transmittances t_i of the inks and superpositions of inks (colorants) are determined respectively according to formula (5) and (6) by measuring the respective reflectances of a white patch and of the solid colorant patches. For 3 inks, respectively 4 inks, this last step requires measuring the reflection spectra of 8, respectively 16 solid colorant patches . Secondly, the scalar initial thicknesses of the inks composing a colorant are deduced by minimizing a difference metric of colorant transmittances predicted according to formula (10) and colorant transmittances deduced from measurements according to the previous step. This second step is only a computation step and requires no additional measurements. Thirdly, halftone patches are printed in all superposition conditions, their reflectances are measured and their effective surface coverages are deduced in order to create the functions mapping nominal to effective surface coverages. For 3 inks or 4 inks, we have 12, respectively 32 different superposition conditions. If we only measure patches at 50% nominal surface coverages, only 12, respectively 32 measurements need to be carried out. Therefore, in total, the calibration of the thickness variation enhanced spectral prediction model requires in case of 3 inks measuring the reflection spectra of 20 patches, and in case of 4 inks, the reflection spectra of 48 patches.

In order to obtain accurate thickness variations, one may first try to obtain the thickness variation factors for the print which is used as calibration print. At first, one may think that since the print is used for the calibration, the thickness variation factors should be exactly one. However, this is not the case, since the initial ink thicknesses are computed with solid patches, whereas the ink thickness variations are deduced from halftone patches. These mean ink thickness variation factors on the reference print, between 0.95 to 1.05, are then used to normalize the ink thickness variations of the prints with modified ink flows.

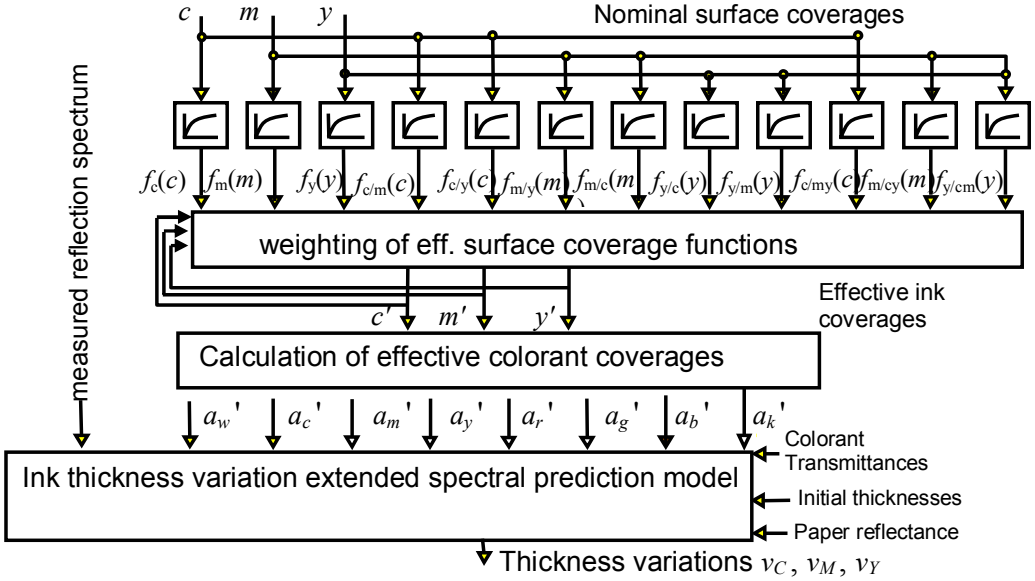

Figure 4. Ink thickness variations deduction framework.

After performing the calibration of the thickness variation enhanced spectral prediction model, the model is ready to be used for deriving the 3, respectively 4 ink thickness variation coefficients. Figure 4 shows the full ink thickness variation deduction framework.

7. Test of the ink thickness variation deduction framework

The proposed ink thickness variation deduction framework is tested in the context of web-offset printing. The pages comprising the calibration patches and the test patches are printed on uncoated newsprint paper, with classical mutually rotated clustered-dot screens, at a screen frequency of 100 lines per inch.

Besides printing the reference sheet with the calibration and test patches, the test also comprises printing the same patches by applying variations to the ink flow. The press operator may specify for each ink either the nominal ink flow, an increased ink flow (~15% increase: "+") or a reduced ink flow (~15% decrease: "-").

Table 4 shows the variants that have been printed. In order to verify the print quality, we create for each of these prints a corresponding ink spreading enhanced Clapper-Yule spectral prediction model and verify the reflectance prediction accuracy. This allows checking the quality of each of the prints, before calibrating the model for deducing ink thickness variations. This is especially important on web offset printers, where there is one ink feed device per vertical stripe (a stripe size on Wifag's press is 35.2 mm wide).

Table 4. Tested variations of the ink flow and corresponding Clapper-Yule spectral prediction accuracy.

Name	DeltaE94Mean	DeltaE94Max	Nb. of patches ΔE_{94}>3
Nominal	1.80886	5.48231	230
C+	1.30492	4.28926	45
C+ M+	1.2755	5.0967	23
M+ Y+	1.45038	6.43138	62
Y+	1.46516	5.77974	57
Y+ K+	1.51478	6.92158	99
K+	1.46979	5.9536	49
C+ K+	1.39565	5.1963	31
C+ M+ K+	1.63454	5.25341	153
C+ M+ Y+ K+	1.57569	5.70446	77
M- K+	1.98473	5.60363	318
C- M- K+	1.4077	5.79149	40
C- K+	1.85632	6.23486	232
C-	1.35127	5.40225	45
C- M-	1.31696	5.81384	50
M-	1.3236	5.12528	36
M- Y-	1.30715	4.520887	34
Y-	1.25692	4.80376	21
Y- K-	1.22929	5.05115	23
K-	1.30306	5.5574	31
C- K-	1.18101	5.10196	21
C- M- K-	1.20744	4.53485	28
C- M- Y- K-	1.14065	5.30539	41

Since the prediction accuracy of the nominal print is low (ΔE_{94}=1.8), we take as reference print for the calibration of the model the print with an increased black ink flow (K+), which has a representative prediction accuracy (mean color difference between prediction and measurement: ΔE_{94}=1.47). This (K+) print is used to deduce the transmittances of the inks, the initial ink thicknesses and the nominal to effective surface coverage functions in all superposition conditions.

We deduce for the other prints the ink thickness variations separately for each patch of the considered set of patches. The first set comprises 317 CMY patches well distributed across the color space. The second set comprises 1529 CMYK patches including the 317 CMY patches of the first set. 73 % of the patches comprising the black ink have surface coverages of black in the range between 5% and 50%. For both sets of patches, we compute the mean thickness variation as well as the corresponding standard deviations.

The presently used difference metric for obtaining the scalar ink thickness variation v_i of each ink i is the sum of square differences between the predicted reflection density spectrum $D_p(\lambda) = -\log_{10}(R_p\ (\lambda))$ and the measured reflection density spectrum $D_m(\lambda) = -\log_{10}(R_m\ (\lambda))$. Using density spectra has the advantage of giving a high weight to low reflectances and a low weight to high reflectances.

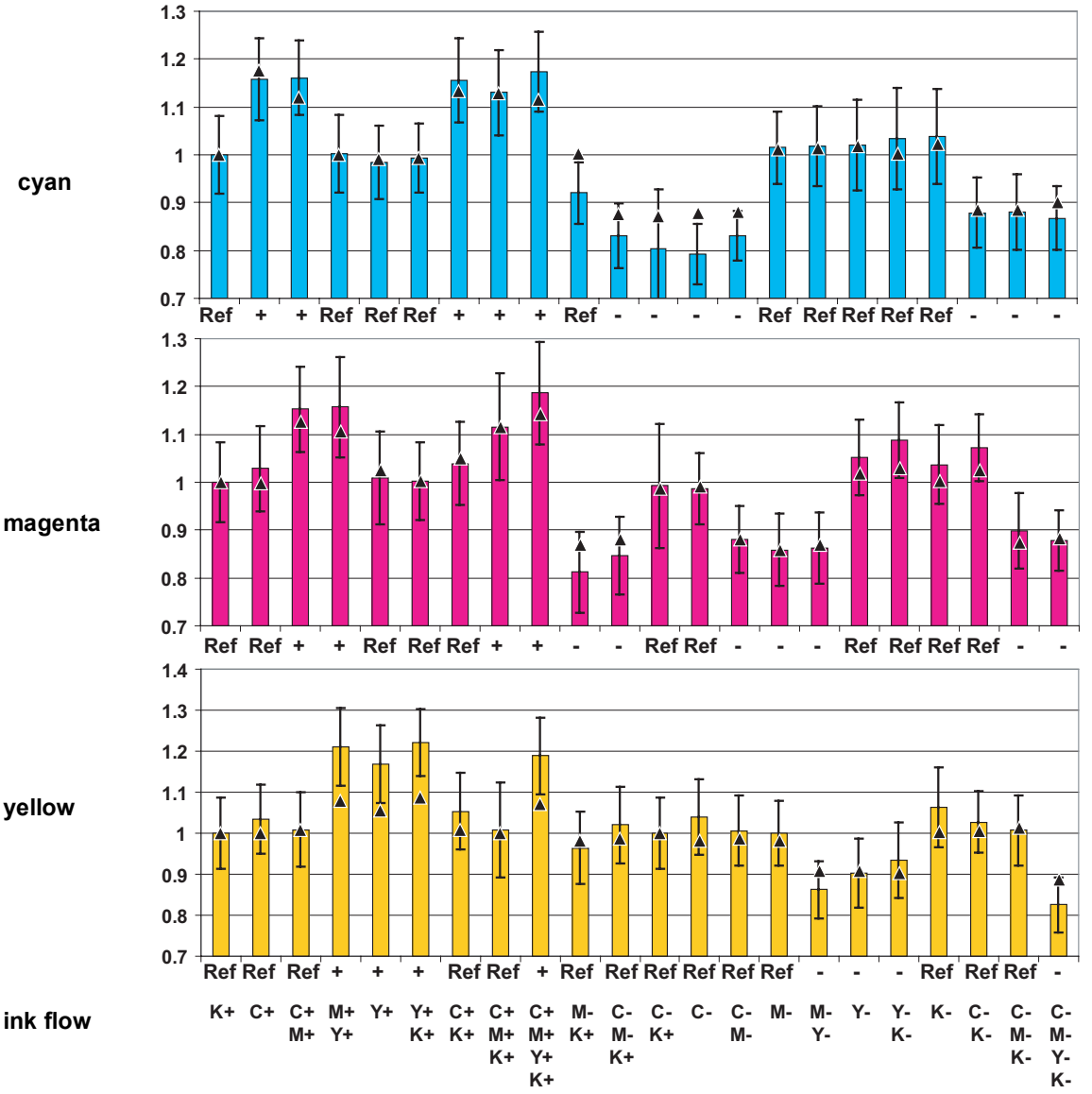

Figure 5. Deduced mean ink thickness variations for prints when varying the ink flows. Each print comprises 317 *cmy* patches distributed across the color space. The interval bars represent the standard deviations and the small triangles represent the density variations of the corresponding solid ink patches.

The predicted ink thickness variations are compared with relative variations of the measured densities of solid printed patches located at the borders of the printed page (small triangles in Figures 5 and 6). This gives a good indication of the agreement between the deduced ink thickness variations and the classical way of obtaining the ink volume variation by measuring the reflection density of a solid ink patch. Each vertical bar corresponds to a different setup of the ink flow.

Figure 5 shows that all increased ink flows (C+, M+ or Y+) yield a mean thickness variation larger than 1.1. The reference ink flows yield a mean ink variation factor between 0.95 and 1.08. Decreased ink flows of cyan, magenta or yellow inks yield decreasing thickness variation factors, generally below 0.90.

Figure 6 shows the results for the second set of patches comprising the cyan, magenta, yellow and black prints, comprising the preceding 317 *cmy* only patches as well as 1212 *cmyk* patches incorporating a certain proportion of black ink. The thickness variation of the cyan and magenta inks are similar as the ones in Figure 5, but with a larger standard deviation. The even larger standard deviation of the yellow ink thickness variation factors (Figure 6) indicates that halftones incorporating superpositions of yellow and black inks are less stable, i.e. the ink mixture varies from one halftone to the next.

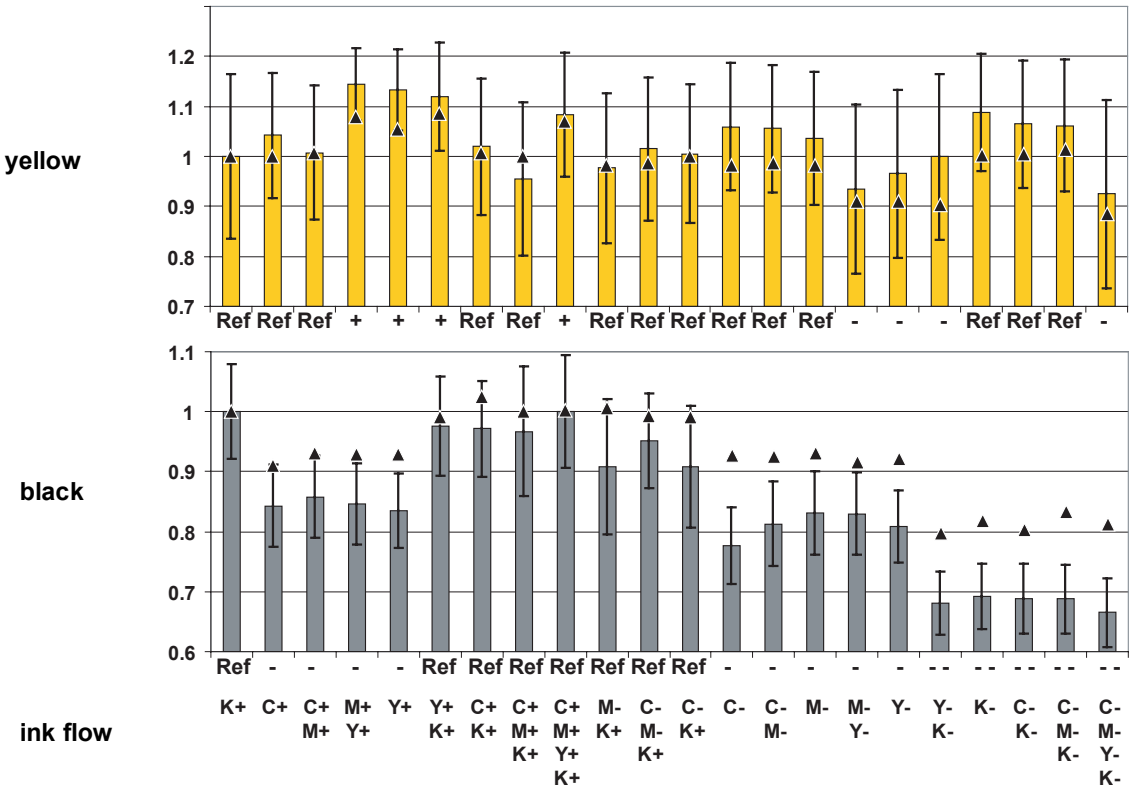

Figure 6. Deduced mean ink thickness variation of the yellow and black inks for a set of 1529 patches per print, together with their standard deviation and the corresponding density variation of solid ink patches. Fitting of thickness variations is performed by considering both the visible and the near infra-red wavelength range (380nm to 850nm).

Since the calibration has been performed on the print with the increased black ink flow (K+), the increased black ink flow expresses the reference ink flow. The reference black ink flow yields a thickness variation factor between 0.9 and 1, the decreased black ink flow (-) yields thickness variation factors between 0.75 and 0.85 and the strongly decreased black ink flow (--) yields thickness variation factors between 0.65 and 0.70. The density variations of the solid black ink are less pronounced than the black ink thickness variations computed from color halftone patches.

The quality of the deduced ink thickness variations can be also verified by inserting for each print its corresponding modified ink thicknesses into the spectral prediction model and by comparing predicted patch reflectances with the measured patch reflectances. For patches printed with the 3 *cmy* inks, the resulting mean prediction accuracy for the C+ print (Table 3) is ΔE_{94}=1.72. For patches printed with the 4 *cmyk* inks, the mean prediction accuracy for the C+ print is ΔE_{94}= 1.93. These values can be compared with the "optimal predictions" obtained by calibrating the thickness enhanced spectral prediction model on the same C+ print (Table 3, for 3 inks, ΔE_{94}=1.31 and for 4 inks, ΔE_{94}=1.63). The slight prediction degradation between the

"optimal predictions" and the predictions with the fitted ink thickness variations are due to the fact that the whole model is calibrated on another print (here the K+ print).

As a general conclusion, ink thickness variations of the cyan, magenta, yellow and black inks can be clearly detected from chromatic halftone patches. We remarked that stopping and restarting the offset press changes slightly the operating conditions. Modifying the operating conditions yields a modified bias for the ink thickness variations. For example, in our experiment, we stopped and restarted the press before the last six ink flow variation experiments. This had the effect of slightly raising the bias of the ink thickness variations, as shown in Figures 5 and 6, for the cyan, magenta and yellow inks.

8. CONCLUSIONS

Offset printing presses are generally controlled by human operators. Control patches located at the borders of the printed page are either manually or automatically measured and corresponding correcting actions are carried out. The presence of control patches often results in a waste of paper and requires additional cutting steps in order to remove them from the final print product. The present research is a first step towards the automatic regulation of inks in printers by relying on the reflectance of multi-chromatic halftones present within the printed pages.

The Clapper-Yule spectral prediction model is the only classical spectral halftone reflection prediction model incorporating explicit expressions for the ink transmittances. By extending it in order to account for ink spreading in all superposition conditions, we obtain accurate spectral reflection predictions. In order to incorporate into the spectral prediction model the notion of ink thickness, we further extend it by expressing colorant transmittances with the transmittances of the corresponding inks raised to the power of their respective initial thicknesses.

Thanks to this ink thickness enhanced Clapper-Yule model, we deduce from a single halftone patch reflectance the respective thickness variations of the contributing inks. Since many different halftones are present within each printed page (gray separation bars, color images), mean thickness variations may be deduced from several halftones and lead to a robust appreciation of the variations in the deposited ink volumes. Cyan, magenta, yellow and black ink thickness variations can be tracked. However, stopping and restarting the printing press may yield a small bias in the deduced ink variation factors.

At present, we consider one full calibration for each combination of papers, inks and screening technology. Further research is being carried out in order to reduce the calibration effort upon change of the print materials or parameters, e.g. for easily adjusting the calibration to different papers, inks and screen frequencies.

REFERENCES

R. Balasubramanian.1999. Optimization of the spectral Neugebauer model for printer characterization, *Journal of Electronic Imaging*, Vol. 8, No. 2, 156-166

F. Brunner. 1989. Method of operating an autotypical color offset machine, US Pat. 4,852,485 issued Aug. 1, 1989.

Th. Bugnon, M. Brichon, R.D. Hersch. 2007. Model-Based Deduction of CMYK Surface Coverages from Visible and Infrared Spectral Measurements of Halftone Prints, , IS&T/SPIE Electronic Imaging Symposium, Conf. Color Imaging XII: Processing, Hardcopy, and Applications, Proc. SPIE Vol. 6493, paper 649310.

M.E. Demichel. 1924. Procédé, Vol. 26, 17-21.

F.R. Clapper and J.A.C Yule. 1953. The effect of multiple internal reflections on the densities of halftone prints on paper, *Journal of the Optical Society of America*, Vol. 43, 600-603

P. Emmel. 2003. Physical models for color prediction, *Digital Color Imaging*, (Ed. G. Sharma), CRC Press, 2003, 173-238

R.D. Hersch and F. Crété. 2005. Improving the Yule-Nielsen modified spectral Neugebauer model by dot surface coverages depending on the ink superposition conditions, IS&T/SPIE Electronic Imaging Symposium, Conf. Imaging X: Processing, Hardcopy and Applications, SPIE Vol. 5667, 434-445

R.D. Hersch, P. Emmel, F. Crété and F. Collaud. 2005. Spectral reflection and dot surface prediction models for color halftone prints, *J. of Electronic Imaging*, Vol. 14, No. 3, 33001-12

E. Hecht. 1974. *Schaum's Outline of Optics*, Mc-Graw-Hill.

K. Iino, R.S. Berns. 1998. Building color management modules using linear optimization I. Desktop, *Journal of Imaging Science and Technology*, Vol. 42, No. 1, 79-94

D.B. Judd. 1942. Fresnel reflection of diffusely incident light, *Journal of Research of the National Bureau of Standards,* Vol. 29, 329-332.

H. Kipphan. 2001. *Handbook of Print Media*. Springer-Verlag,

H.E.J. Neugebauer. 1989. Die theoretischen Grundlagen des Mehrfarbendrucks. *Zeitschrift fuer wissenschaftliche Photographie,* Vol. 36, 36-73, (1937), reprinted in *Neugebauer Seminar on Color Reproduction,* SPIE Vol-1184,194-202.

G. Rogers. 2000. A Generalized Clapper-Yule Model of Halftone Reflectance. *Journal of Color Research and Application,* Vol. 25, No. 6, 402-407

J.L. Saunderson. 1942. Calculation of the color pigmented plastics, *Journal of the Optical Society of America*, Vol. 32, 727- 736

M. Shaw, G. Sharma, R. Bala, E.N. Dalal. 2003. Color printer characterization adjustment for different substrates, *Journal of Color Research and Application*, Vol. 28, No. 6, 454-467

J.A.S Viggiano. 1990. Modeling the Color of Multi-Colored Halftones, Proc. TAGA, 44-62

X.X. Wang, R. Nemeth. 1995. Ink separation device for printing press ink feed control, US Pat. 5,903,712, filed Oct. 5, 1995, issued May 11, 1999

D.R.Wyble, R.S. Berns. 2000. A Critical Review of Spectral Models Applied to Binary Color Printing, *Journal of Color Research and Application*, Vol. 25, No. 1, 4-19

J.A.C. Yule and W.J. Nielsen. 1951. The penetration of light into paper and its effect on halftone reproductions, Proc. *TAGA*, Vol. 3, 65-76

APPENDIX

Table A. Relative ink thicknesses of superpositions of the cyan, magenta, yellow inks with the black ink, fitted in respect to a wavelength range of 380nm to 850nm, for the K+ reference print (Table 4).

black	cyan/black		magenta/black		yellow/black		cyan/magenta/black		
d_K	d_{Ck}	d_{cK}	d_{Mk}	d_{mK}	d_{Yk}	d_{yK}	d_{Cmk}	d_{cMk}	d_{cmK}
1	0.336	0.975	0.387	0.900	0.194	0.954	0.363	0.221	0.896

cyan/yellow/black			magenta/yellow/black			cyan/magenta/yellow/black			
d_{Cyk}	d_{cYk}	d_{cyK}	d_{Myk}	d_{mYk}	d_{myK}	d_{Cmyk}	d_{cMyk}	d_{cmYk}	d_{cmyK}
0.510	0.222	0.817	0.377	0.097	0.877	0.508	0.243	0.169	0.7768